ACS APPLIED MATERIALS & INTERFACES

Research Article

www.acsami.org

Dielectric Breakdown in Silica–Amorphous Polymer Nanocomposite Films: The Role of the Polymer Matrix

Christopher A. Grabowski,[†] Scott P. Fillery,[‡,§] Nicholas M. Westing,[§] Changzai Chi,[⊥] Jeffrey S. Meth,[⊥] Michael F. Durstock,[§] and Richard A. Vaia*[,§]

[†]UES, Inc., Dayton, Ohio 45432, United States

[‡]National Research Council, Washington, D.C. 20001, United States

[§]Materials and Manufacturing Directorate, Air Force Research Laboratory, Wright Patterson Air Force Base, Ohio 45433-7750, United States

[⊥]DuPont Nanocomposite Technologies and DuPont Central Corporate Analytical Services, Central Research & Development, E.I. DuPont de Nemours & Co., Inc., Wilmington, Delaware 19880-0400, United States

Supporting Information

ABSTRACT: The ultimate energy storage performance of an electrostatic capacitor is determined by the dielectric characteristics of the material separating its conductive electrodes. Polymers are commonly employed due to their processability and high breakdown strength; however, demands for higher energy storage have encouraged investigations of ceramic–polymer composites. Maintaining dielectric strength, and thus minimizing flaw size and heterogeneities, has focused development toward nanocomposite (NC) films; but results lack consistency, potentially due to variations in polymer purity, nanoparticle surface treatments, nanoparticle size, and film morphology. To experimentally establish the dominant factors in broad structure–performance relationships, we compare the dielectric properties for four high-purity amorphous polymer films (polymethyl methacrylate, polystyrene, polyimide, and poly-4-vinylpyridine) incorporating uniformly dispersed silica colloids (up to 45% v/v). Factors known to contribute to premature breakdown—field exclusion and agglomeration—have been mitigated in this experiment to focus on what impact the polymer and polymer–nanoparticle interactions have on breakdown. Our findings indicate that adding colloidal silica to higher breakdown strength amorphous polymers (polymethyl methacrylate and polyimide) causes a reduction in dielectric strength as compared to the neat polymer. Alternatively, low breakdown strength amorphous polymers (poly-4-vinylpyridine and especially polystyrene) with comparable silica dispersion show similar or even improved breakdown strength for 7.5–15% v/v silica. At ∼15% v/v or greater silica content, all the polymer NC films exhibit breakdown at similar electric fields, implying that at these loadings failure becomes independent of polymer matrix and is dominated by silica.

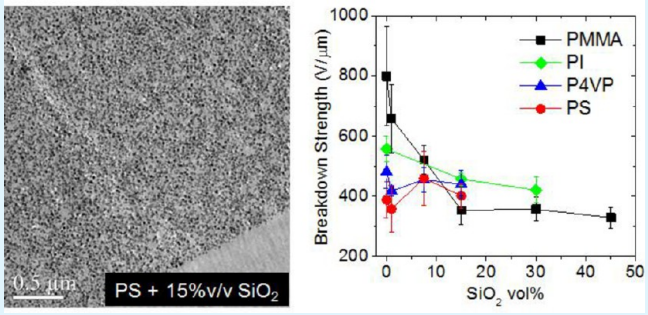

KEYWORDS: *polymer nanocomposite, colloidal silica, dielectric breakdown, dielectric strength, permittivity, energy storage*

INTRODUCTION

The demand for improved energy storage solutions has driven the development of power conditioning and management devices that endure higher operating voltages with greater reliability. For pulsed power applications, electrostatic capacitors have a distinct advantage over fuel cells and batteries given their rapid electrical discharge/storage capabilities.[1] Their use though is limited by their comparatively low energy densities, which impedes efforts to reduce device weight and size. The maximum energy an electrostatic capacitor can store is dependent on the dielectric permittivity and dielectric strength of the insulating material separating the electrodes. For instance, commonly used polymer dielectric BOPP (biaxially oriented polypropylene) has a relatively high breakdown strength E_{BD} of ∼600 V/μm for large scale production films; however, due to its low permittivity (ε_r = 2.2), maximum theoretical energy density ($u = 1/2\varepsilon_o\varepsilon_r|E_{BD}|^2$) is limited to 4 J/cm^3 and including device packaging, practical performance is less than 2 J/cm^3. Dielectric polymer nanocomposites (PNCs) have been proposed as alternatives in an effort to significantly improve capacitor performance and create more efficient devices that occupy less space.[1−5]

The key goal for PNC dielectric design is to avoid failure, and thus, the overwhelming drive has been to improve nanoscale morphology of the nanoparticle fillers to minimize heterogeneities.[4,6] In parallel, use of high permittivity metal oxide

Received: February 11, 2013
Accepted: April 15, 2013
Published: April 15, 2013

nanoparticles, such as $BaTiO_3$ or TiO_2, affords direct routes to improve permittivity.[7−12] Since energy density has a quadratic dependence on field strength, the dielectric permittivity must be dramatically improved by the nanoparticles to offset any reduction in breakdown properties. Finite difference simulations have shown that increased loadings of $BaTiO_3$ nanoparticles monotonically reduces breakdown strength of a polymeric host material, up to a 50% reduction in E_{BD} for 40% v/v $BaTiO_3$.[6,10] This behavior was explained by the formation of percolation networks of the randomly dispersed particles at high loadings. These networks create electrical pathways that prematurely break down the composite. Experimentally, uniform dispersions at such high volume fractions are very difficult to achieve and more often than not are accompanied by agglomerate formation, which act like defect sites and further reduce dielectric strength. Furthermore, field exclusion from the high permittivity inclusions generates large localized fields within the polymer matrix. Experimental studies confirm that even moderate (5−10% v/v) $BaTiO_3$ nanoparticle loaded materials create electric field distributions with localized "hot spots", which negatively impact dielectric strength.[13] In general, therefore, it is very challenging to separate the individual contributions of field exclusion and sample morphology to dielectric breakdown.

Composite materials that incorporate permittivity matching fillers (such as silica and clay) can help diminish field exclusion as an experimental factor and provide insight to the impact of morphology on breakdown. For example, cross-linked polyethylene showed an increase in dielectric strength from 269 to 314 V/μm for an addition of 5% w/w silica nanoparticles.[14,15] Polypropylene showed breakdown enhancement from 511 to 778 V/μm at similarly low silica volume fractions (<1% v/v).[16] In concert, researchers have found that the size of the filler critically influences the dielectric strength—samples loaded with micrometer-sized inclusions tended to fail at far lower applied fields as compared to both silica PNCs and neat polymer films.[15] Some speculate that the relative improvement of electrical breakdown properties results from a more uniform electric field distribution within thin films.[17] Others speculate that the improvement is associated with a "barrier" effect that can be optimized through morphology control. Interwoven structures have been theoretically proven to prolong breakdown occurrence by forcing the electric field to travel a more tortuous path.[21] Experimentally, films built from alternating nanolayers of high dielectric constant poly(vinylidene fluoride) (PVDF) and high breakdown strength polycarbonate have enhanced breakdown strength, generated by the presence of barriers that hinder the propagating electric field.[18,19] Nanolaminates formed from organically modified montmorillonite (oMMT) mixed with polyvinyl butyral (PVB) have shown improved breakdown strength for volume fractions as high as 25% v/v oMMT, increasing E_{BD} from 100 V/μm (neat film) to as high as 130 V/μm (10% v/v oMMT).[23] Others have shown enhanced breakdown of oMMT-polyethylene nanocomposites when the filler material adopts long-range alignment. E_{BD} was measured at 300 V/μm for neat polymer films, while 6% w/w films exhibited breakdown at 290 (random) and 370 V/μm (aligned).[22] These enhancements are consistent with reports of other matrices (nylon, polyester, low-density polyethylene, and PVDF) containing 1−5% w/w oMMT.[20,24] In summary, it is clear that filler composition, size, and morphology are important considerations for PNC dielectric performance, but it is difficult to conclude what is the role of the polymer matrix, including chemical structure, polarity or morphology, and habit or fraction of crystallites. Furthermore, since dispersibility is directly related to the polymer−nanoparticle interface, it has been equally difficult to separately examine nanoparticle surface treatments while maintaining morphology and polymer crystal structure (and vice versa).

To better understand these issues for nanoscale composites, we compare the dielectric permittivity and dielectric strength measurements of four electronic-grade amorphous polymers: polymethyl methacrylate (PMMA), polystyrene (PS), polyimide (PI), and poly-4-vinylpyridine (P4VP) containing up to 45% v/v highly dispersed colloidal silica. Overall, we find that incorporation of silica nanoparticles in high dielectric strength amorphous polymers (PMMA and PI) show marked reduction in breakdown strength, even in low (1% v/v) loadings. Alternatively, nanocomposites produced using lower dielectric strength amorphous polymers (P4VP and PS) retain or enhance their breakdown strength up to 15% v/v silica. These findings demonstrate that polymer nanocomposite concepts have the most promise as potential low-cost solutions for improving amorphous polymers that exhibit poor breakdown properties, especially when the additive properties imparted by the particulate filler, such as heat deflection and flammability suppression, are also desired.

EXPERIMENTAL METHODS

Silica Nanocomposite Film Preparation. Polymethyl methacrylate (PMMA, 600 000 M_W Aldrich) was dissolved in methylethylketone (MEK), filtered through Celite, and reprecipitated into methanol. Polystyrene (PS, 400 000 M_W, Pressure Chemical) was dissolved in MEK, filtered through Celite, and then reprecipitated into methanol. Poly(4-vinylpyridine) (P4VP, Aldrich, 65 000 M_W) was dissolved in MEK, filtered through Celite, and reprecipitated into methanol. The polyimide (PI) was derived from PMDA/ODA (pyromellitic dianhydride/oxidianiline) polyamic acid solution in DMAC that was converted to the polyimide at 400 °C. The colloidal silica employed was Ludox AS-40 (Aldrich) which had been solvent transferred into DMF. Particle diameter is 29 nm, with a polydispersity of 0.11.[25] For dispersion into the polystyrene and polyimide host matrices, the colloidal silica was treated with a phenyltrimethoxysilane (Aldrich) capping agent to afford ∼1.5 phenyl groups per squared nanometer of silica surface area. Phenyl group density was determined by size exclusion chromatography. When passing the dispersion over a column, the unattached capping agents pass through the column after the capped silica. The relative amount of attached and unattached capping agents was measured via UV absorbance of the eluent; this was compared to the amount of capping agent initially present in the reaction to calculate graft density. For the PMMA and P4VP matrices, uncapped silica with its native hydroxyl surface functionality was used.

PNCs were prepared following previously published procedures.[25] In brief, the colloidal silica dispersion in DMF was mixed with a 10 wt % polymer solution in DMF and mixed on a jar roller for at least 3 days. This formulation was coated using a 6 mil doctor blade onto 7 in. × 7 in. aluminum coated glass, heated to 100 °C (aluminum thickness was 500 nm). This resulted in films that were 5−10 μm in thickness, as measured by stylus profilometry (Tencor P-10). The aluminum acted as the bottom electrode of the capacitor structure.

To perform transmission electron microscopy (TEM), the appropriate formulation was first coated onto a Kapton substrate and dried with the same procedure used for the samples on aluminum coated glass. A layer of unfilled PMMA or PS (depending on the sample) was laminated to the sample as an encapsulant to protect the sample from the potting compounds used in TEM preparation. The laminate was then potted and microtomed to produce a sample with cross-section of ∼90 nm in thickness.

Dielectric and Electrical Characterization. Dielectric breakdown studies were performed by employing a custom-built device that

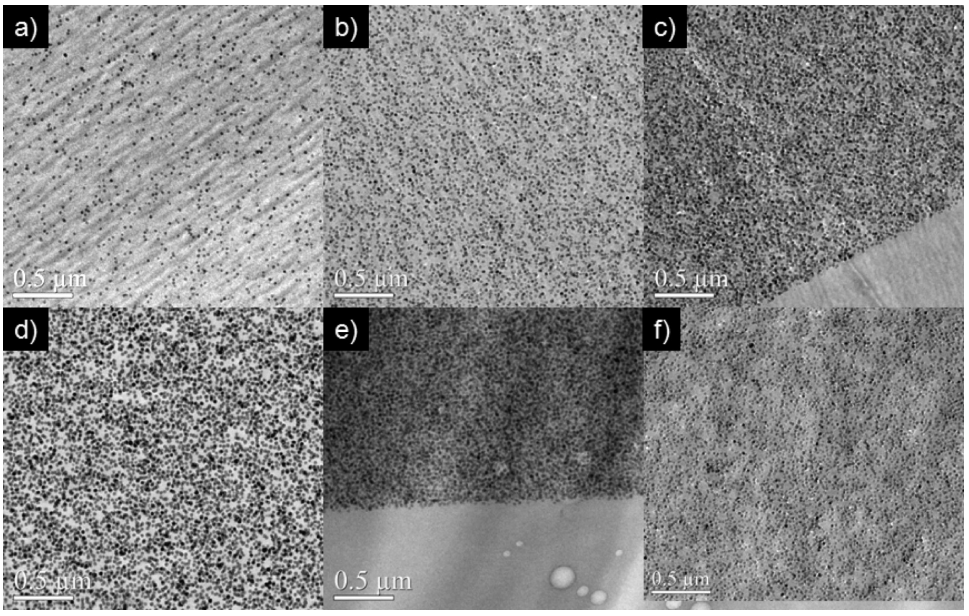

Figure 1. Representative TEM images of PNC films at various silica loading. (a–c) Polystyrene films with 1, 7.5, and 15% v/v silica loading, respectively. (d–f) 15% v/v nanocomposite films using PMMA, P4VP, and polyimide as host matrix, respectively. Scale bars correspond to 0.5 μm.

features a 10 kV Spellman SL300 high voltage supply. The power supply is coupled to a ramping circuit set to 300 V/s for all trials. This corresponds to a breakdown event occurring at ∼20 s, which is an acceptable value under the ASTM standard protocol for short-term dielectric strength tests.[26] The breakdown voltage was recorded for each sample using a Fluke 289 multimeter, set in peak capture mode. A silicon controlled rectifier switch triggers once >1 mA current is detected passing through the sample; the voltage when this event occurs was deemed the breakdown voltage.

The breakdown experiments utilized two experimental geometries. In the first method, a copper rod with a hemispherical end (radius of curvature = 2.5 mm) makes direct contact with the PNC film. This experimental geometry examines a confined sample region (area ∼0.1 cm^2), in an attempt to remove any influence of film heterogeneity due to processing by spatially localizing the electric field. The alternate geometry sandwiches a Kapton mask (thickness 70 μm) with a 1 cm diameter circular opening between the film and a piece of metalized BOPP. Here, the area under investigation is much larger (0.784 cm^2), and the recorded dielectric strengths were characteristically 15–30% lower due to a higher probability of probing larger sample flaws (see Figure S1, Supporting Information). At least 15 breakdown trials were performed for each film to conduct Weibull failure analysis. The copper contact rod was polished after every 15 breakdowns using diamond paste to remove pitting, Kapton masks were cleaned after 15 trials to prevent edge erosion from impacting results, and the metalized BOPP film was replaced after every trial.

Free-standing BOPP film was periodically employed as a test standard to ensure our experimental platform remained calibrated. Values obtained for characteristic dielectric strength were $E_{BD} \sim 700$ V/μm for 0.784 cm^2 sample areas and 800 V/μm (0.1 cm^2 sample area), which are comparable to results previously reported in literature.[27] All experiments were conducted at room temperature in an N_2 purged environment where relative humidity was observed in the range of 20–30%. Breakdown voltages were converted to breakdown strength by measuring film thickness near each test site via profilometry.

Dielectric impedance and permittivity measurements were conducted on all PNC films using a Novocontrol Alpha Analyzer. A circular aluminum contact 1 cm in diameter and 200 nm thick was deposited onto each film, whereupon a drop of colloidal silver was placed to prevent damage to the aluminum film. Thin needle probes rested on the colloidal silver contact points to facilitate the measurements, which were conducted in an N_2 purged environment at room temperature. Permittivity was measured at discrete frequencies, swept over the range 0.1 Hz to 100 kHz at an AC driving voltage of 1 V.

Leakage current measurements were conducted using a 10 kV Spellman SL300 power supply and Keithley 6517B electrometer. Sample contact utilized the same geometry described for permittivity studies. Voltage was applied at 100 V increments and held for 30 s. The reported leakage currents were measured at 50% of the characteristic breakdown voltage. To remove effects caused by sample dielectric time constant, all current values are the average of the final 2 s of voltage hold. Current density was calculated by dividing by contact area.

RESULTS AND DISCUSSION

The four amorphous polymers discussed have comparable permittivities (PS 2.6, PMMA 3.0, PI 3.3, P4VP 3.6 at 100 kHz) but range in characteristic dielectric strength from 400 (PS) up to 800 V/μm (PMMA). Use of highly purified electronic grade amorphous polymers is crucial to minimize potential for breakdown dominated by impurity derived carriers. The relatively close permittivity match between the silica nanoparticles and surrounding amorphous polymer limits field enhancement effects and more directly tests how dielectric breakdown is influenced by polymer–colloid interactions. Figure 1 shows representative TEM images of the polymer–silica nanocomposites created by the previously reported solvent route.[25] The use of polar nonaqueous solvents such as dimethylformamide (DMF) and dimethylacetamide (DMAC), during composite formation, forestalls aggregation by enabling charge stabilization of the colloidal silica. Coating the polymer–silica formulation onto a hot glass plate (∼100 °C) enhances the drying rate, further suppressing aggregation due to kinetic factors. By the time sufficient solvent has evaporated such that the colloidal silica loses its charge stabilization, the matrix viscosity is high enough to prevent significant particle diffusion, resulting in highly dispersed PNCs. As seen, this approach yielded highly dispersed silica with a morphology that is qualitatively similar across all four polymer matrices even up to high silica fractions (>15% v/v).

The real dielectric permittivity of PNC films, measured at 100 kHz frequency, is plotted in Figure 2 as a function of silica loading (see Figure S2, Supporting Information, for full frequency scans). Permittivity for 0% v/v films, which corresponds to neat polymer films, was 2.6 for PS, 2.8 for PMMA, 2.9 for PI, and 3.3 for P4VP. These measured values match to within ±10% of values reported in the literature.[28] The permittivity generally increases monotonically for higher loadings of silica, which is expected since silica has a higher permittivity and reasonably follows Bruggeman model estimates (shown as lines) assuming silica permittivity ε_{SiO2} = 4.5. The imaginary permittivity component, measured at 1 Hz and 100 kHz for each sample, is also plotted in Figure 2. All NCs exhibit increased dissipation with increased silica loading in a similar manner relative to the dielectric loss of the base polymer. A noted exception is PS, which exhibits more sensitivity to silica addition, albeit the unfilled PS has the lowest loss of the base polymers. All the PMMA materials show the highest imaginary permittivity ($\varepsilon'' \sim 0.1$ at 100 kHz; 0.2–0.8 at 1 Hz), whereas all other materials have $\varepsilon'' < 0.1$. Low loss at low field, such as from impedance spectroscopy, is a reasonable metric for high field behavior, as dissipative processes are related to leakage currents, which facilitate electron cascading and thus premature breakdown.

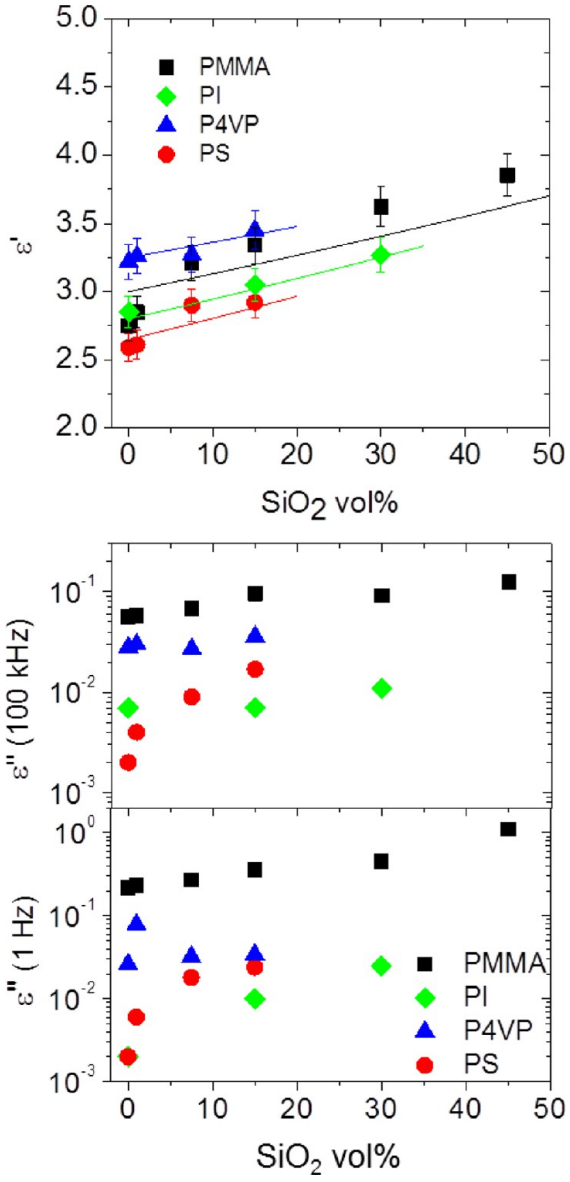

Figure 2. (top) Real dielectric permittivity component (ε') measured at 100 kHz frequency of PNC films as a function of silica volume fraction. Error bars represent uncertainty in film thickness and impedance measurement reproducibility. Straight lines correspond to Bruggeman model estimates, assuming silica permittivity is ε_{SiO2} = 4.5. Similar trends for permittivity were observed at 1 kHz frequency. (bottom) Imaginary dielectric permittivity component (ε'') measured at 100 kHz and 1 Hz frequency.

Figure 3 displays the probability for dielectric failure of silica-loaded PMMA films as an example of results for the four

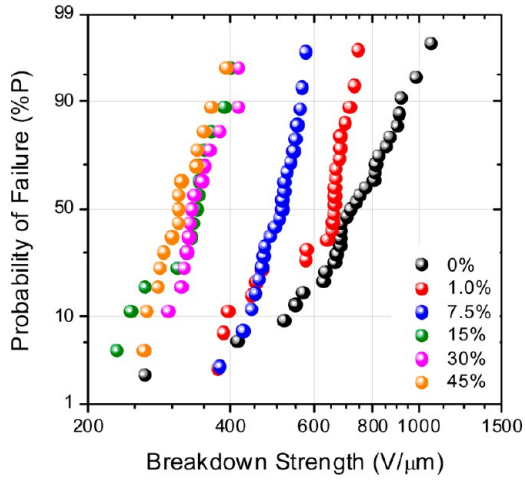

Figure 3. Probability of failure for PMMA PNC films with increasing percent v/v silica loading. Tests were performed utilizing the probe-contact experimental geometry (see Experimental Methods section). Twenty-five individual breakdown tests were conducted for the 0, 1, 7.5% v/v loadings, while 15 tests were conducted for 15, 30, and 45% v/v loadings.

amorphous polymer matrices (see Figures S3–S5, Supporting Information for other breakdown data). Figures 4 and 5 summarize our analysis of PNC failure utilizing a two-parameter Weibull cumulative probability function: $P(E) = 1-\exp[-(E/E_{BD})^{\beta}]$, where $P(E)$ is the cumulative probability for electric failure and E is experimentally recorded breakdown strength. The fitting parameters are E_{BD}, the characteristic breakdown strength (i.e., the breakdown field where there is 63.2% probability for failure), and β, the shape parameter associated with the least-squares linear fit of the distribution. Results reported in Figures 3, 4, and 5 are for the copper rod measurement geometry outlined in the experimental procedure. Corresponding E_{BD} results for the geometry utilizing metalized BOPP were ~15–30% smaller, but followed similar trends (see Figure S1, Supporting Information).

While prior studies have shown that small loadings of silica increase breakdown for polyethylene and polypropylene films, Figure 4 demonstrates that the breakdown of silica–polymer NCs depends greatly on the chemical nature of the amorphous polymer matrix. PMMA is significantly impacted by even small amounts of colloidal silica, reducing breakdown strength from 800 V/μm for a neat film down to 350 V/μm at 15% v/v loading. Higher loadings in the range of 15–45% v/v show relatively little change in dielectric strength for PMMA. PI also shows reduction in E_{BD}, but at a smaller decline, from 560

dx.doi.org/10.1021/am4005623 | ACS Appl. Mater. Interfaces 2013, 5, 5486–5492

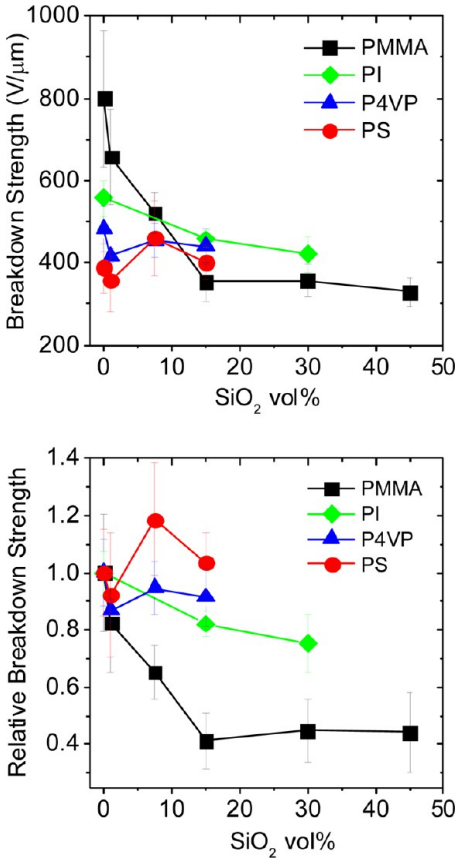

Figure 4. (top) Characteristic breakdown strength (E_{BD}) of PNC films as a function of silica volume fraction. E_{BD} is determined at 63.2% failure probability from a two-parameter linear Weibull failure analysis. Error bars represent one standard deviation of the E_{BD} values measured across >15 breakdown tests. (bottom) Characteristic breakdown strength of PNC films relative to the neat polymer as a function of silica volume fraction.

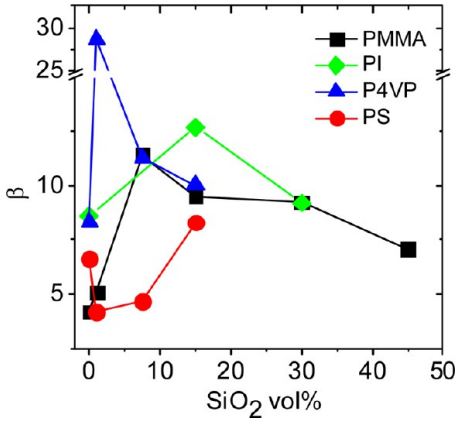

Figure 5. Shape parameter (β) from a two-parameter linear Weibull failure analysis of PNC films as a function of silica volume fraction.

(neat) down to 460 V/μm (15% v/v). P4VP has even less change in E_{BD} than PI, with values of 480 (neat) down to 440 V/μm (15% v/v). In marked contrast, PS, the polymer that displayed the poorest E_{BD} (390 V/μm, neat) demonstrated enhanced breakdown strength at 7.5% v/v and 15% v/v loadings (460 and 400 V/μm, respectively). All four nanocomposites have comparable dielectric strength (7.5% v/v 450−530 V/μm and 15% v/v 350−450 V/μm) for intermediate to high silica nanoparticle loading, suggesting that silica becomes a dominant factor for dielectric failure once volume fractions reach 7.5−15%. Note that these trends do not reflect the general low-field dissipative behavior; in that PS and PI have similar loss. Also, this behavior does not track the high field leakage current, whereas silica volume fraction increases, all the PNCs show increased current density at 50% of breakdown field (see Figure S6, Supporting Information). PMMA and PS PNCs (i.e., opposite breakdown trends with silica loading) have comparable current densities. Furthermore, the breakdown trends do not reflect the surface treatment of the silica. PS and PI utilize phenyltrimethoxysilane treated silica but exhibit opposite behavior with increasing silica loading. Likewise, PMMA and P4VP containing silica with a native hydroxyl surface exhibit different trends. Thus, the surface treatment of the silica is not a direct first-order effect on the experimental results. This is important to note as surface functionalization and particle coatings are discussed as a means to improve breakdown properties of PNC films, but conclusive evidence of their role in enhancing dispersion (morphology) or creating trap or scattering states has been elusive.[12,29,30] Overall therefore, these results imply that adding silica nanoparticles at any level of loading to higher breakdown amorphous polymer films (PMMA and PI) tends to reduce dielectric strength. Conversely, amorphous polymers with poorer breakdown properties (P4VP and especially PS) appear to be mostly unaffected and can even show up to 20% dielectric strength improvement for moderate silica loading. Finally at the highest loadings the dielectric strength of all the systems converge, most likely reflecting the response of the filler.

Providing a physical description that explains the breakdown trends in these amorphous PNCs is not straightforward and open to interpretation. We shall outline two related concepts which are self-consistent with our observed results. Since failure converges toward similar values for all PNCs with increasing silica loading, breakdown may be initiated by the silica colloids themselves in our composite. If silica inherently breaks down at a designated electric field, this would suppress the dielectric strength in PMMA and PI PNCs. This inherent silica breakdown strength must be ∼450 V/μm−lower than neat PMMA and PI but higher than neat PS. Given the sensitivity of failure measurements to experimental protocols, these values are in the general range of other reports of improved dielectric strength in PNCs featuring silica-loaded amorphous polypropylene[16] (neat E_{BD} ∼ 500 V/μm). However, for amorphous matrices such as PS, where the breakdown characteristics are less than that implied for silica, it is unclear why this weaker polymer matrix mechanism would be suppressed by the replacement of a small fraction of material with higher inherent failure characteristics, since failure is initiated from the most susceptible flaws, which is still the majority (i.e., the PS matrix). This would imply that silica impacts the propagation of failure, rather than initiation. Thus, the implication is that well-dispersed silica can serve as a positive (e.g., forestalls propagation) or negative (e.g., induces failure) performance additive depending on the *relative* breakdown characteristics of the silica and the matrix and not on any absolute characteristic of the silica or its surface.

The question remains as to what is the critical relative characteristic? As a possibility, the trends may be understood based on the relative polarity of silica to the polymer matrix. Comparing the dielectric constant (ε) and measured E_{BD} of the neat polymer films (Figure 4), we observe that the least polar

polymer (PS) has the lowest breakdown strength and the most polar polymer (PMMA) has the highest. At this point it is important to recall that the silica−polymer nanocomposites under consideration are amorphous—specifically chosen to minimize complexity and exclude the impact of silica addition to crystallite formation, as well as the role of crystallites in dielectric failure. Nonpolar dielectric polymers that exhibit relative high breakdown are semicrystalline, such as BOPP, and their performance is dominated by their crystalline morphologies (and not polarity of amorphous regions). For electronic grade amorphous polymers, high breakdown strength has been previously associated with polar polymers, including the observation that breakdown strength increases for nonpolar polyethylene upon introduction of polar groups such as C−O.[31] The presence of polar groups is thought to act as additional scattering centers or charge trapping sites through the formation of highly stable defects.[32] When adding silica nanoparticles to nonpolar amorphous polymers such as polystyrene, low-density polyethylene, and polypropylene, breakdown improvement is consistent with the polar surface of silica providing stable sites to trap or scatter charge within the film. This effectively inhibits propagation and forestalls breakdown to higher fields if the surface of the silica (modified or native) is more polar than the matrix. This stand-off capability is also consistent with prior voltage endurance studies of silica and layered aluminosilicate filled polymers, where the increase in voltage endurance was greater for less polar matrices.[20] Conversely though, in highly polar polymers such as PMMA, the polar surface of silica (native or modified) affords less stable trap sites than inherent in the polymer. As such, silica acts as a defect which fails at lower fields compared to the surrounding matrix, providing a lower energy alternative to the superior properties of the polar moieties along the polymer backbone. Finally at high volume fractions, the surface area of silica becomes sufficient to dominate breakdown characteristics, and thus, the failure of the nanocomposites becomes independent of the matrix. It is interesting to note that this occurs around 15% v/v loading, close to the percolation threshold for spheres in three dimensions.[33,34]

Consistent with the polarity argument is the general trend in Weibull parameter β (Figure 5) with silica content and polymer matrix. Adding silica to the higher breakdown strength polymers (PMMA, PI, P4VP) reduces variability in dielectric breakdown, characterized by increasing β. The uniform distribution of silica colloids within these polymer films (Figure 1) results in a uniform network of defect sites. Thus, silica decreases breakdown by introducing a lower energy failure mode, but due to its uniform distribution, also reduces failure variability. Note that even though E_{BD} is decreased, increasing the reproducibility of failure by eliminating the probability of failure at low fields has important industrial applications where design is driven by the onset (not mean) failure field. For example, insulation film thickness can be reduced and upper voltage limits can be increased closer to the characteristic breakdown strength for higher β materials because there is less likelihood for failure. In contrast to these films, PS demonstrates increasing failure variability (lower β) for low silica loading (1−7.5% v/v). Relative to the matrix, silica is acting as a trap site rather than a failure site. Thus the effectiveness of silica depends on the probability of a failure event encountering the particle. This will be smallest at low silica concentration and increase with loading. This is reflected in the general trending of β with increased silica in PS. Finally, at silica loading >15% v/v, all PNC films tend to fail with comparable variability. As noted for breakdown at these loadings, silica becomes the overwhelming mode for sample failure and masks host matrix breakdown properties.

CONCLUSIONS AND FUTURE OUTLOOK

Improving the energy storage capabilities of electrostatic capacitors has fostered great interest in engineering composite films that show improved dielectric properties. Outside of the overall scale of the heterogeneities, competing factors control and trigger breakdown events, including field exclusion, agglomeration, and sample morphology. By preparing PNC films that feature a nanofiller dispersed uniformly in a series of electrical-grade, permittivity matching amorphous polymer matrices, we directly investigated the fundamental mechanisms for breakdown in PNCs. Higher breakdown strength amorphous polymers (polymethyl methacrylate and polyimide) exhibited reduced breakdown strength upon adding colloidal silica, while alternatively, low breakdown strength amorphous polymers (poly-4-vinylpyridine and polystyrene) retained or showed enhanced breakdown strength for 7.5−15% v/v silica. These observations are significant because they indicate that to engineer PNC dielectrics the first-order effect is *synergistic between filler and matrix* and not solely determined by the characteristics of the filler surface. Finally, all PNC films loaded with >15% v/v silica displayed similar breakdown characteristics. This result is significant because the four neat amorphous polymers range considerably in dielectric performance (E_{BD} spans 400−800 V/μm), and this implies that addition of silica nanoparticles masks the amorphous polymer's inherent dielectric strength attributes, causing all films to fail during approximately similar conditions at these crucial high-inorganic loadings.

Due to the wide range of breakdown behavior when adding silica, the interactions between amorphous polymer host and nanoparticle that drive PNC film failure must vary substantially. We reason that in lower breakdown amorphous polymers, silica helps to trap or scatter charge, thus enhancing the dielectric strength of the composite system. Conversely, silica has a detrimental effect in higher breakdown amorphous polymers because it presents a lower energy failure mode. A related finding from these experiments is the narrower distribution of failure probability for PNC films that experienced reduced dielectric strength. We speculate this reduction in variability is caused by the high uniformity of defects within the film. Overall, these conclusions provide a heuristic guideline to dielectric PNC design where it is insufficient to control just the nanoparticle morphology and surface, but necessitates the ability to tune the relative polarity of the nanoparticle surface with regard to the matrix while maintaining dispersion. The continuing lack of a definitive fundamental understanding of the initiation and propagation processes in nanocomposite dielectric failure predicates the need for additional studies to differentiate morphology, particle composition, and relative polarity effects. Nevertheless, the comparison of PMMA, PS, P4VP, and PI reinforces that such general insight cannot be derived from studies of one matrix with different nanoparticle fillers at increasing volume fraction, but must simultaneously examine size, composition, source, and surface chemistry of the nanoparticle in an expanded range of host polymer matrices.

We conclude from these results that breakdown performance in amorphous polymers with E_{BD} < 400 V/μm may be improved by adding well-dispersed colloidal silica in moderate

amounts (up to 15% v/v). Furthermore, the reduction in breakdown variability observed in some films may prove beneficial for industrial applications where more reliable/predictable components are required. Finally, as more technologies arise that demand multifunctionality from constituent materials, discussions presented here can be extended to predict how breakdown may be potentially impacted for composite materials that also have demands for simultaneous mechanical, thermal, and/or dielectric enhancement.

■ ASSOCIATED CONTENT

Supporting Information

Dielectric permittivity scans for all PNCs, full breakdown data, and comparing breakdown results for different sample geometries. This material is available free of charge via the Internet at http://pubs.acs.org.

■ AUTHOR INFORMATION

Corresponding Author

*E-mail: Richard.Vaia@wpafb.af.mil.

Notes

The authors declare no competing financial interest.

■ ACKNOWLEDGMENTS

The authors wish to thank the Air Force Office of Scientific Research and Air Force Research Laboratory Materials & Manufacturing Directorate for their financial support.

■ ABBREVIATIONS

polymer nanocomposite = PNC
biaxially oriented polypropylene = BOPP
poly(vinylidene fluoride) = PVDF
organically modified montmorillonite = oMMT
polymethyl methacrylate = PMMA
polystyrene = PS
polyimide = PI
poly-4-vinylpyridine = P4VP
dimethylformamide = DMF
dimethylacetamide = DMAC
methylethylketone = MEK
pyromellitic dianhydride/oxidianiline = PMDA/ODA
transmission electron microscopy = TEM

■ REFERENCES

(1) Wang, Q.; Zhu, L. *J. Polym. Sci. B Polym. Phys.* **2011**, *49*, 1421−1429.
(2) Nelson, J. *Dielectric Polymer Nanocomposites*; Springer: New York, 2010.
(3) Ducharme, S. *ACS Nano* **2009**, *3*, 2447−2450.
(4) Barber, P.; Balasubramanian, S.; Anguchamy, Y.; Gong, S.; Wibowo, A.; Gao, H.; Ploehn, H. J.; zur Loye, H. C. *Materials* **2009**, *2*, 1697−1733.
(5) Cao, Y.; Irwin, P. C.; Younsi, K. *IEEE Trans. Dielectr. Electr. Insul.* **2004**, *11*, 797−807.
(6) Calame, J. P. *J. Appl. Phys.* **2006**, *99*, 084101.
(7) Nelson, J. K.; Fothergill, J. C. *Nanotechnology* **2004**, *15*, 586−595.
(8) Dang, Z.-M.; Lin, Y.-Q.; Xu, H.-P.; Shi, C.-Y.; Li, S.-T.; Bai, J. *Adv. Funct. Mater.* **2008**, *18*, 1509−1517.
(9) Jung, H. M.; Kang, J.-H.; Yang, S. Y.; Won, J. C.; Kim, Y. S. *Chem. Mater.* **2010**, *22*, 450−456.
(10) Kim, P.; Doss, N. M.; Tillotson, J. P.; Hotchkiss, P. J.; Pan, M.-J.; Marder, S. R.; Li, J.; Calame, J. P.; Perry, J. W. *ACS Nano* **2009**, *3*, 2581−2592.
(11) Tuncer, E.; Sauers, I.; James, D. R.; Ellis, A. R.; Paranthaman, M. P.; Goyal, A.; More, K. L. *Nanotechnology* **2007**, *18*, 325704.
(12) McCarthy, D. N.; Stoyanov, H.; Rychkov, D.; Ragusch, H.; Melzer, M.; Kofod, G. *Compos. Sci. Technol.* **2012**, *72*, 731−736.
(13) Li, J. Y.; Zhang, L.; Ducharme, S. *Appl. Phys. Lett.* **2007**, *90*, 132901.
(14) Roy, M.; Nelson, J. K.; MacCrone, R. K.; Schadler, L. S.; Reed, C. W.; Keefe, R.; Zenger, W. *IEEE Trans. Dielectr. Electr. Insul.* **2005**, *12*, 629−643.
(15) Roy, M.; Nelson, J. K.; MacCrone, R. K.; Schadler, L. S. *J. Mater. Sci.* **2007**, *42*, 3789−3799.
(16) Takala, M.; Ranta, H.; Nevalainen, P.; Pakonen, P.; Pelto, J.; Karttunen, M.; Virtanen, S.; Koivu, V.; Pettersson, M.; Sonerud, B.; Kannus, K. *IEEE Trans. Dielectr. Electr. Insul.* **2010**, *17*, 1259−1267.
(17) Lewis, T. J. *IEEE Trans. Dielectr. Electr. Insul.* **2004**, *11*, 739−753.
(18) Mackey, M.; Hiltner, A.; Baer, E.; Flandin, L.; Wolak, M. A.; Shirk, J. S. *J. Phys. D Appl. Phys.* **2009**, *42*, 175304.
(19) Wolak, M. A.; Wan, A. S.; Shirk, J. S.; Mackey, M.; Hiltner, A.; Baer, E. *J. Appl. Polym. Sci.* **2012**, *123*, 2548−2557.
(20) Brandstetter, S. S.; Drummy, L. F.; Horwath, J. C.; Schweickart, D. L.; Vaia, R. A. Breakdown Voltage of Thermoplastics with Clay Nanometer-Sized Fillers. *Proceedings of the 2008 IEEE International Power Modulators and High Voltage Conference*, Las Vegas, NV, May 27−31,2008; pp 287−290
(21) Vogelsang, R.; Farr, T.; Frohlich, K. *IEEE Trans. Dielectr. Electr. Insul.* **2006**, *13*, 373−382.
(22) Tomer, V.; Polizos, G.; Randall, C. A.; Manias, E. *J. Appl. Phys.* **2011**, *109*, 074113.
(23) Fillery, S. P.; Koerner, H.; Drummy, L.; Dunkerley, E.; Durstock, M. F.; Schmidt, D. F.; Vaia, R. A. *ACS Appl. Mater. Interfaces* **2012**, *4*, 1388−1396.
(24) Tomer, V.; Manias, E.; Randall, C. A. *J. Appl. Phys.* **2011**, *110*, 044107.
(25) Meth, J. S.; Zane, S. G.; Chi, C. Z.; Londono, J. D.; Wood, B. A.; Cotts, P.; Keating, M.; Guise, W.; Weigand, S. *Macromolecules* **2011**, *44*, 8301−8313.
(26) ASTM D 149 Standard Test Method for Dielectric Breakdown Voltage and Dielectric Strength of Solid Electrical Insulating Materials at Commercial Power Frequencies. In *Annual Book of ASTM Standards, American Society for Testing and Materials*; ASTM: Conshohocken, PA, 1992.
(27) Laihonen, S. J.; Gafvert, U.; Schutte, T.; Gedde, U. W. *IEEE Trans. Dielectr. Electr. Insul.* **2007**, *14*, 275−286.
(28) Brandup, J.; Immergut, E. H.; Grulke, E. A.; Bloch, D. *Polymer Handbook*, 4th ed.; Wiley: New York, 1999.
(29) Siddabattuni, S.; Schuman, T. P.; Dogan, F. *Mater. Sci. Eng. B Adv. Funct. Mater.* **2011**, *176*, 1422−1429.
(30) Fredin, L. A.; Li, Z.; Ratner, M. A.; Lanagan, M. T.; Marks, T. J. *Adv. Mater.* **2012**, *24*, 5946−5953.
(31) Oakes, W. G. *Proc. IEEE* **1949**, *96*, 37−43.
(32) Seanor, D. A. *Electrical Properties of Polymers*; Academic Press, Inc.: Orlando, 1982.
(33) Scher, H.; Zallen, R. *J. Chem. Phys.* **1970**, *53*, 3759−3761.
(34) Wu, K.; Dissado, L. A.; Okamoto, T. *Appl. Phys. Lett.* **2004**, *85*, 4454−4456.